

Time-Dependent Influence of Hypoxic Ischemic Encephalopathy in Cerebral Metabolite Changes in Neonatal Rats Detected by In vivo 1H MR Spectroscopy at 9.4 T

Do-Wan Lee^{1,2}, Dong-Cheol Woo², Minyoung Lee^{2,3}, Chul-Woong Woo², Sang-Tae Kim², Choong Gon Choi⁴, Bo-Young Choe¹, and Byong Sop Lee³
¹Department of Biomedical Engineering, and Research Institute of Biomedical Engineering, The Catholic University of Korea College of Medicine, Seoul, S eoul, Korea, ²Asan Institute for Life Sciences, Asan Medical Center, Seoul, Seoul, Korea, ³Department of Pediatrics, Asan Medical Center, University of Ul san College of Medicine, Seoul, Korea, ⁴Department of Radiology, Asan Medical Center, University of Ulsan College of Medicine, Seoul, Korea

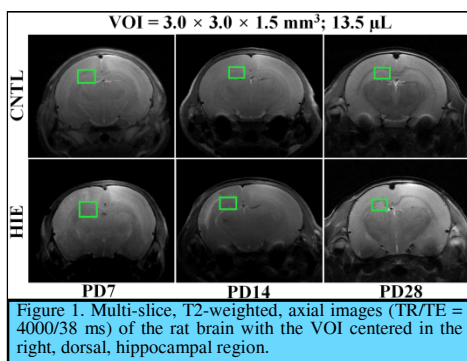


Figure 1. Multi-slice, T2-weighted, axial images (TR/TE = 4000/38 ms) of the rat brain with the VOI centered in the right, dorsal, hippocampal region.

acquired from the same voxel (averages = 8). We conducted the time course scan from which all MR images and ¹H spectra were acquired at PD7, PD14, and PD28 from the right hippocampal region after the PD7 HIE modeling procedure, and using the same imaging and spectroscopic parameters. The obtained *in vivo* ¹H-MR spectra images were processed according to the LCModel. This method permitted the calculation of metabolite concentrations from a fit to the experimental spectrum, and based on a simulated basis set. The following brain metabolites were included in the basis set: alanine (Ala); aspartate (Asp); creatine (Cr); γ -aminobutyric acid (GABA); glucose (Glc); glutamate (Glu); glutamine (Gln); glutathione (GSH); glycerophosphorylcholine (GPC); phosphorylcholine (PCh); myo-inositol (mIns); lactate (Lac); phosphocreatine (PCr); scyllo-inositol (sIns); *N*-acetylaspartate (NAA); *N*-acetylaspartylglutamate (NAAG); taurine (Tau); assorted macromolecules; and assorted lipids. Absolute metabolite concentrations (mmol/kg wet weight) were calculated using unsuppressed water signals as internal references, assuming an 88% (PD7), 85% (PD14) or 80% (PD28 and more) brain water concentration³. The *in vivo* proton spectra were judged to be within an acceptable range based on the Cramer-Rao lower bound (CRLB) which gives an estimate of the standard deviation (SD) of the fit for each metabolite. Only those metabolites with a CRLB of <50% in at least half of spectra were reported and used for analyses. Metabolite concentrations with a CRLB of \geq 50% were regarded as not detected/validated.

Results: Figure 2 shows the representative *in vivo* ¹H-MRS spectra acquired from the right, dorsal, hippocampal region of the HIE rats. All metabolite signals were quantified using the LCModel, with a simulated basis set. *In vivo* ¹H-MRS spectra were assigned to the resulting 16, cerebral metabolite signals. Eighteen metabolite

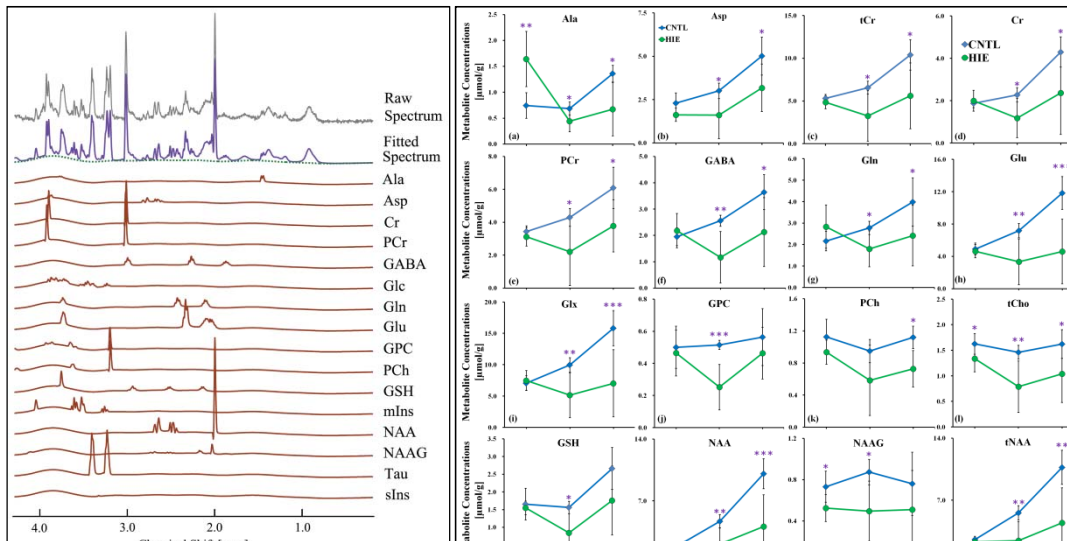


Figure 2. Representative *in vivo* ¹H MR spectra acquired at 9.4 T in the hippocampal region of stress-induced, sleep-perturbed rats. Quantified spectra are represented by several colors, as follows: Fitted spectra (purple); raw spectrum (grey); baseline (dotted green); and metabolite signals (red).

signals from all *in vivo* ¹H spectra were visualized and analyzed below than in 50 of the %SD (CRLB: Cramér-Rao-lower-bounds). Figure 3 illustrates the changes of the cerebral metabolite concentrations that were quantified from the *in vivo* ¹H-MRS spectra at PD7, PD14, and PD28 of the CNTL and HIE rats. Independent t-tests revealed that a total of 16 metabolite signals in the HIE rats were significantly altered with increased periods of the development, compared to the CNTL. Figure 4 indicates that the shaded areas demonstrate differences in the metabolite concentration between the CNTL and the HIE rats at three, significant levels in the region of the dorsal hippocampal region.

Discussion and Conclusion: We demonstrated the time-dependent influence of HIE in neuropathological metabolite changes in the neonatal rat brain, using *in vivo* ¹H MR spectroscopy at 9.4 T. Our results showed that the numerous markers of brain damage in the HIE model were significantly altered compared to the CNTL, and possibly due to post-ischemic and hypoxic injuries. We also found a varying pattern of the neurochemical responses in the HIE model of developing brain with increasing time (at PD7, PD14, and PD28). According to our results and those of previous studies⁵, the present study is unique in that we discovered not only the usefulness of traditional markers (NAA, Cr, and choline-containing compounds, etc.) but also several new results (Ala, Asp, Glu, Gln, and GSH, etc.) from a neonatal rat model of severe HIE. The determination of the reliable markers of the extent and severity of ischemic and hypoxic injuries will be crucial for the appropriate selection of HIE newborns selected for neuroprotective therapy. Future studies using histochemical and molecular methodologies in HIE rat brain with a regional quantification are required in order to strengthen our findings.

References: 1. Rice JE, Vannucci RC, Brierley JB. Ann. Neurol. 1981;9:131–141., 2. Cansev M, Minbay Z, Goren B, et al., Neurosci. Lett. 2013;542:65–70., 3. Cheong JLY, Cady EB, Penrice J, et al., Am. J. Neuroradiol. 2006;27:1546–1554., 4. Tkac I, Rao R, Georgieff MK, et al., Magn. Reson. Med. 2003;50:24–32., 5. Lee BS, Woo CW, Kim ST, et al., Pediatr. Res. 2010;68:303–308.

Target audience: Neurologists, psychiatrists, and clinicians interested in MRS of the brain disorders.

Purpose: Brain damage as a consequence of combined injury caused by hypoxia and reduced cerebral blood flow (ischemia) in fetuses and newborn infants, is a major cause of cerebral palsy, mental retardation, and epilepsy¹. Moreover, neonatal hypoxic ischemic encephalopathy (HIE) is a major cause of permanent brain injury with significant consequences including a neurological impairment and changes of the cerebral metabolites^{2,3}. The purpose of this study was to quantitatively assess and determine the influence of the time-dependent effects of the HIE on cerebral metabolite changes in a neonatal rat model of severe HIE.

Methods: Fourteen, male, Sprague-Dawley rats were divided into two groups, i.e. control (CNTL: n = 6) and hypoxic ischemic encephalopathy rats (HIE: n = 8)]. Surgical procedures in the HIE rat model were performed on postnatal day (PD) seven rats. The right, common carotid artery was carefully ligated using 5/0 silk following a midline incision. After a 60-min recovery period, all HIE rats were placed in a chamber maintained at a temperature of 36°C and were exposed to humidified 8% oxygen for 150 min. After a 15-min recovery period, T2-weighted and ¹H magnetic resonance spectroscopy (¹H-MRS) images were acquired using a 9.4T/160-mm animal MRI system. For the voxel localization (Fig. 1), T2-weighted MR images were acquired (slice thickness = 1 mm, matrix = 256 x 256). All ¹H-MRS spectra images were acquired through a signal voxel in the right dorsal hippocampal region of the brain using the point-resolved spectroscopy (PRESS) sequence for 256 acquisitions with TR/TE = 5000/13.4 ms. For quantification, the unsuppressed water signals were also

acquired from the same voxel (averages = 8). We conducted the time course scan from which all MR images and ¹H spectra were acquired at PD7, PD14, and PD28 from the right hippocampal region after the PD7 HIE modeling procedure, and using the same imaging and spectroscopic parameters. The obtained *in vivo* ¹H-MR spectra images were processed according to the LCModel. This method permitted the calculation of metabolite concentrations from a fit to the experimental spectrum, and based on a simulated basis set. The following brain metabolites were included in the basis set: alanine (Ala); aspartate (Asp); creatine (Cr); γ -aminobutyric acid (GABA); glucose (Glc); glutamate (Glu); glutamine (Gln); glutathione (GSH); glycerophosphorylcholine (GPC); phosphorylcholine (PCh); myo-inositol (mIns); lactate (Lac); phosphocreatine (PCr); scyllo-inositol (sIns); *N*-acetylaspartate (NAA); *N*-acetylaspartylglutamate (NAAG); taurine (Tau); assorted macromolecules; and assorted lipids. Absolute metabolite concentrations (mmol/kg wet weight) were calculated using unsuppressed water signals as internal references, assuming an 88% (PD7), 85% (PD14) or 80% (PD28 and more) brain water concentration³. The *in vivo* proton spectra were judged to be within an acceptable range based on the Cramer-Rao lower bound (CRLB) which gives an estimate of the standard deviation (SD) of the fit for each metabolite. Only those metabolites with a CRLB of <50% in at least half of spectra were reported and used for analyses. Metabolite concentrations with a CRLB of \geq 50% were regarded as not detected/validated.

Results: Figure 2 shows the representative *in vivo* ¹H-MRS spectra acquired from the right, dorsal, hippocampal region of the HIE rats. All metabolite signals were quantified using the LCModel, with a simulated basis set. *In vivo* ¹H-MRS spectra were assigned to the resulting 16, cerebral metabolite signals. Eighteen metabolite

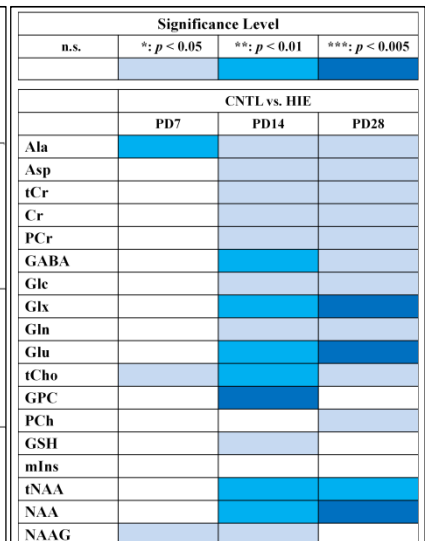


Figure 3. Alterations of the cerebral metabolite concentrations in the hippocampal region between the CNTL and the HIE rats at PD7, PD14, and PD28. The vertical lines on each of the clusters indicate the (\pm) standard deviation of the mean values. Significance levels (independent t-test): *p < 0.05; **p < 0.01; ***p < 0.005.

Figure 4. Schematic representation of the differences in metabolite concentrations between the CNTL and the HIE rats, in the region of the dorsal hippocampal region. Significance levels (independent t-test): *p < 0.05; **p < 0.01; ***p < 0.005.